Publ. Astron. Soc. Japan (2019) 71 (3), 58 (1–13)
doi: 10.1093/pasj/psz034
Advance Access Publication Date: 2019 April 21

Stellar wind accretion and accretion disk formation: Applications to neutron star high-mass X-ray binaries

Shigeyuki KARINO,[1,*] Kenji NAKAMURA,[2,*] and Ali TAANI[3,*]

[1]Faculty of Science and Engineering, Kyushu Sangyo University, 2-3-1 Matsukadai, Higashi-ku, Fukuoka, Fukuoka 813-8503, Japan
[2]Department of Mechanical Engineering, Kyushu Sangyo University, 2-3-1 Matsukadai, Higashi-ku, Fukuoka, Fukuoka 813-8503, Japan
[3]Physics Department, Faculty of Science, Al-Balqa Applied University, 19117 Salt, Jordan
*E-mail: karino@ip.kyusan-u.ac.jp (SK), nakamura@ip.kyusan-u.ac.jp (KN), ali.taani@bau.edu.jo (AT)

Received 2018 November 9; Accepted 2019 March 1

Abstract

Recent X-ray observations have revealed the complexity and diversity of high-mass X-ray binaries (HMXBs). This diversity challenges a classical understanding of the accretion process on to the compact objects. In this study, we reinforce the conventional concept of the nature of wind-fed accretion on to a neutron star considering the geometrical effect of radiatively accelerated wind, and re-evaluate the transported angular momentum by using a simple wind model. Our results suggest that even in an OB-type HMXB fed by stellar wind, a large amount of angular momentum could be transported to form an accretion disk due to the wind-inhomogeneity, if the binary separation is tight enough and/or the stellar wind is slow. We apply our model to actual systems such as LMC X-4 and OAO 1657−415, and discuss the possibility of disk formations in these systems.

Key words: accretion, accretion disks — stars: neutron — X-rays: binaries — X-rays: individual (LMC X-4, OAO 1657−415)

1 Introduction

X-ray binary systems involving neutron stars are classified into two classes, according to their donor mass: high-mass X-ray binaries (HMXBs) and low-mass X-ray binaries (LMXBs). Among them, HMXBs are further classified into OB-type and Be-type (Corbet 1984, 1986; Bhattacharya & van den Heuvel 1991; Bildsten et al. 1997; Pfahl et al. 2002) according to the type of the donor. In general, in an OB-type system a neutron star captures quasi-spherical wind matter ejected by a massive donor. In this case, the accretion geometry around the neutron star takes an almost spherical Bondi flow (Hoyle & Lyttleton 1939; Bondi & Hoyle 1944). If the accreting compact object is a *magnetized* neutron star, accreted matter would be captured by the magnetosphere at a certain radius. It is generally considered that the quasi-spherical accretion flow could be trapped by the strong magnetic field of a neutron star before the formation of an accretion disk in an OB-type HMXB. With the recent growth in the number of observed systems, however, the diversity of the accretion mode in HMXBs has been revealed and peculiar systems which do not follow the traditional understanding have been found (Walter et al. 2015). For instance, the accretion modes in supergiant fast X-ray transients (SFXTs) are still under active discussion: several

theories have been verified such as clumpy wind accretion, a magnetic gating mechanism due to a strong field, and/or a settling spherical accretion shell (in't Zand 2005; Walter & Zurita Heras 2007; Bozzo et al. 2008; Shakura et al. 2014). Furthermore, recently, discussions about the accretion and emission mechanisms of pulsating ultra-luminous X-ray sources involving neutron stars have been started (Bachetti et al. 2014; Ekşi et al. 2015; Fürst et al. 2016; Israel et al. 2017a, 2017b).

Although the study of OB-type HMXBs which are persistent, bright X-ray sources has a long history, the nature of OB-type HMXBs has not yet been understood completely. OB-type systems typically have orbital periods of several days, and their X-ray luminosities are relatively persistent. They occupy the upper left-hand region of the Corbet diagram; their spin periods are systematically long even though their orbits are rather shorter than Be-type HMXBs (Corbet 1984, 1986). This means that the transportation rate of the angular momentum via wind accretion is much lower than disk accretion. In general, a spherical Bondi accretion is assumed in the wind-fed X-ray binaries and/or axisymmetric accretion is often considered (Hoyle & Lyttleton 1939; Foglizzo & Ruffert 1997; Edgar 2004). This simplification, however, cannot be valid in certain situations. Especially, in tight binary systems with slow wind, the effect due to the Coriolis force cannot be negligible (Huarte-Espinosa et al. 2013). In such systems, the relative velocity vector of the stellar wind becomes inclined to the binary axis. Furthermore, if the donor is a massive star, the wind matter could be accelerated via the line-driven mechanism (Castor et al. 1975), and there could be a steep gradient in the velocity and density in the radial direction. Due to this inclined accelerated wind, the accretion flow captured by a neutron star could have significant inhomogeneities of density and velocity, as shown in figure 1. These inhomogeneities bring a certain amount of angular momentum on to the accreting neutron star, and if it is large enough, an accretion disk may be formed around the neutron star. Here, we examine the transferred angular momentum due to the inhomogeneity of the stellar wind in tight binary systems and investigate the possibility of the disk formation in wind-fed X-ray binary systems.

In this study, we show that an accretion disk could be formed around the magnetized neutron star even in a wind-fed binary system, when the binary separation is narrow and/or wind velocity is slow. This result will play an important role in the understanding of some peculiarities and diversities of observed HMXBs. We apply our analysis of inhomogeneous wind accretion to actual observed sources as follows: LMC X-4, which is a well-known OB-type HMXB and has an accretion disk around the neutron star and often shows large X-ray flares exceeding the Eddington luminosity (Ilovaisky et al. 1984; Levine et al. 1991; Moon et al. 2003), and OAO 1657−415, which shows peculiar binary parameters that cannot be explained by any binary evolution scenario (Mason et al. 2012). The nature of these systems could somehow be different from the typical figure of OB-type HMXBs fed via stellar wind (Taani et al. 2018, 2019). In past, these systems have been considered to be fed via Roche lobe overflow (RLOF) accretion (Frank et al. 2002). According to recent studies, however, it is suggested that the donors of these systems are rather small and cannot fulfill their Roche lobe (van der Meer et al. 2007; Rawls et al. 2011; Falanga et al. 2015). In addition to this, it is necessary to discuss the stability of the binary system that RLOF mass transfer proceeds from a massive donor to a relatively less-massive neutron star (Eggleton 2006). In order to understand the nature of these peculiar systems, we need to revisit the nature of wind-fed accretion from massive donors. Therefore, we apply our model to these systems, and show that neutron stars in these systems could receive enough angular momentum from the stellar wind to form accretion disks.

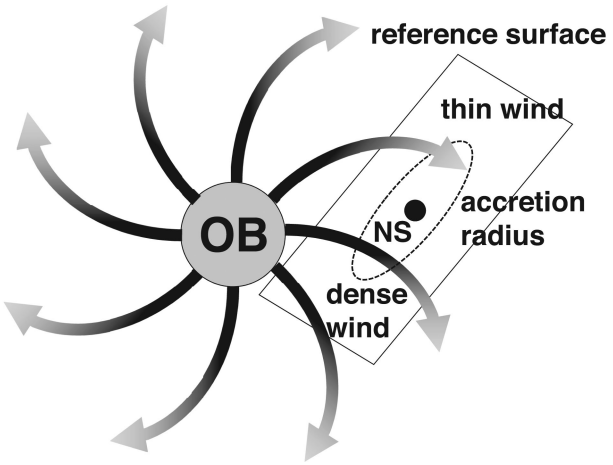

Fig. 1. The situation considered in this study. The density of radiatively accelerated wind rapidly decreases once it has departed from the donor surface. Because of the Coriolis force, the wind could be trailing and hence the accretion matter could have inhomogeneity.

In the next section, we briefly show the method of our analysis. In section 3, we show the results. In section 4, we discuss the validity and limits of our analysis. Then we show some results of further applications to observed systems. The final section is devoted to the conclusion.

2 Transportation of angular momentum via stellar wind

Transportation processes of angular momentum via stellar wind in X-ray binaries have been studied not only by analytical approaches but also by numerical approaches. For

example, in Shapiro and Lightman (1976), the authors suggested that a black hole fed by asymmetric stellar wind can form an accretion disk when the orbital motion is taken into account. On the other hand, they showed that a neutron star cannot have an accretion disk since the inner radius of the disk is too small. Their work had been extended to investigate the spin-up/down evolution of a compact accreting object fed by stellar wind by Wang (1981). Angular momentum transportation via non-uniform stellar wind has been studied numerically by many authors, and especially since the 1990s, where the numerical simulations of wind accretion on to compact objects have been actively studied (Theuns & Jorissen 1993; Ruffert & Anzer 1995; Ruffert 1999; Blondin & Pope 2009). After the notable findings of the flip-flop instability in the supersonic accretion flows (Matsuda et al. 1987; Fryxell & Taam 1988), systematic studies have been carried out (Matsuda et al. 1991; Ruffert 1997, 1999). Highly resolved wind computations have revealed that, under certain conditions, the angular momentum of the asymmetric wind could be transported to the circumference of the accreting object, and an accretion disk could be formed (Blondin & Pope 2009; Blondin 2013). Furthermore, when the wind is dense and slow, such as the slow wind emanating from giant/asymptotic giant branch donors, it is suggested that a static accretion disk could be formed without the flip-flop behavior (Theuns & Jorissen 1993; Soker 2004; Huarte-Espinosa et al. 2013). Several such hydrodynamical studies of the interaction between a giant donor and compact accretor have been performed, covering a wide range of phenomena (Jahanara et al. 2005; Hadrava & Čechura 2012; Liu et al. 2017; El Mellah & Casse 2017). In these works, however, they have not supposed a *magnetized* neutron stars as an accreting object.

On the other hand, in the context of X-ray binaries with OB-type donors, (quasi-)spherical wind accretion is considered in most cases (Shakura et al. 2012; Postnov et al. 2016); it is considered that the angular momentum is rather *withdrawn* from the neutron star due to the interaction between the neutron stellar field and the wind matter (Davies & Pringle 1981; Bozzo et al. 2008; Giménez-García et al. 2016). However, in most of previous studies, the line-acceleration of the wind from the OB-type donor (Castor et al. 1975) is omitted, except for some simple analyses (Wang 1981). The rapid acceleration produces a steep gradient of the wind velocity and density in the radial direction. When the orbital velocity is comparable to the wind velocity, the relative velocity vector of the wind could be inclined significantly (see figure 1); and this radial gradient of the wind velocity could remarkably eliminate the symmetry of the wind to the accreting object (Huarte-Espinosa et al. 2013).

Hence in this study, we consider wind accretion processes and the consequent angular momentum transport taking such an asymmetry of the wind into account, using the simple wind model. When the orbital motion is comparable to the wind velocity, the stellar wind is no longer symmetric about the binary axis. Additionally, if the stellar wind suffered from line-driven acceleration, the wind density decreases rapidly. As a result of this acceleration, the velocity and density distribution of the stellar wind passing the neutron star neighborhood becomes more asymmetric. These asymmetries bring some amount of angular momentum to the accreting neutron star. In this study, we aim to evaluate the angular momentum transported due to this asymmetry.

In this purpose, we need an orbital radius $R_{\rm orb}$, and we obtain this from the Keplerian law;

$$R_{\rm orb} = \left[\frac{G(M_{\rm d} + M_{\rm NS})P_{\rm orb}^2}{4\pi^2}\right]^{1/3}. \tag{1}$$

Here, we assume that the donor mass is much larger than that of the neutron star ($M_{\rm d} \gg M_{\rm NS}$) and the system takes a circular orbit. In addition, the orbital velocity of the neutron star, $\boldsymbol{v}_{\rm orb} = v_{\rm orb}\boldsymbol{e}_{\rm T}$ can be obtained by

$$v_{\rm orb} = \sqrt{\frac{GM_{\rm d}}{R_{\rm orb}}}. \tag{2}$$

$\boldsymbol{e}_{\rm T}$ denotes a unit vector in the direction of the orbital motion of the neutron star. At the neutron star position ($R_{\rm orb}$), the wind velocity accelerated via line force $\boldsymbol{v}_{\rm w} = v_{\rm w}\boldsymbol{e}_{\rm R}$ is computed by

$$v_{\rm w} = v_{\rm inf}\left(1 - \frac{R_{\rm d}}{R_{\rm orb}}\right)^{\beta}, \tag{3}$$

where $R_{\rm d}$ denotes the radius of the donor (Castor et al. 1975; Kudritzki & Puls 2000). $\boldsymbol{e}_{\rm R}$ denotes a unit vector in the radial direction seen from the center of the donor (see the Appendix). The acceleration parameter β is fixed as $\beta = 1$. $v_{\rm inf}$ denotes the wind velocity at infinity. From equations (2) and (3), the relative velocity between the neutron star and the wind can be obtained as follows:

$$v_{\rm rel}^2 = v_{\rm w}^2 + v_{\rm orb}^2. \tag{4}$$

Here we introduce a reference surface S which includes the neutron star, to evaluate the accretion rate of mass and angular momentum. We set this surface to have its normal vector coincident with the relative velocity vector of the wind, $\boldsymbol{v}_{\rm rel}$, at the neutron star position.

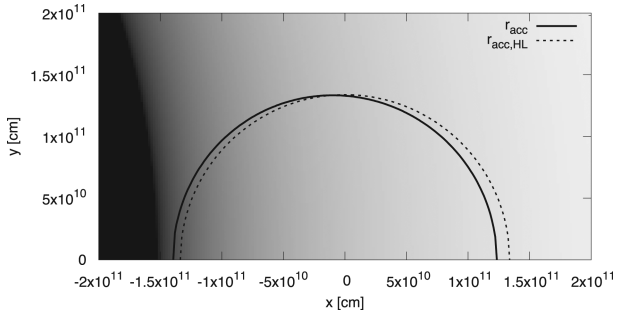

Fig. 2. Oblate accretion area defined by the balance between wind kinetic energy and the neutron star potential is shown by the solid curve. At the same time, the accretion area evaluated from the wind velocity at the neutron star position (hitherto known as the Hoyle–Littleton theory) is shown by the dashed curve. Density of the wind matter is also shown by the gray scale: the dark gray region corresponds to thick wind density. The entire range from the pale end to the dark end covers one order of magnitude of the wind density.

The gravitational potential of the neutron star at each position on the S surface is

$$U = -\frac{GM_{\rm NS}}{r}, \tag{5}$$

where r is the distance from the neutron star on the r surface. If this potential overcomes the kinetic energy of the wind $K = v_{\rm rel}^2/2$, the wind matter passing this point will be trapped by the neutron star. Using an analogy from Hoyle–Littleton accretion theory (Hoyle & Lyttleton 1939; Foglizzo & Ruffert 1997), the area where the accretion matter would be trapped in the reference surface S can be shown by the maximum radius of such an area, $r_{\rm acc}$. The shape of $r_{\rm acc}$ gets distorted depending on the wind and orbital parameters, as shown in figure 2. In this figure, the locus of $U + K = 0$ on the S surface is shown by the solid curve, while an accretion radius evaluated by the wind velocity at the neutron star position is shown by the dashed line (Hoyle–Littleton theory). At the same time, the wind density on the S surface is indicated by the gray value. Clearly, the accretion area defined by $U + K = 0$ shifts toward the dense side. Note that such a deformation of the accretion region has been neglected in previous theoretical works (Hoyle & Lyttleton 1939; Wang 1981; Foglizzo & Ruffert 1997).

The accretion rate of mass and angular momentum given by the accretion matter passing the area $r < r(U + K = 0)$ are computed as

$$\dot{M} = \int_{r<r(U+K=0)} \rho_{\rm w} v_{\rm rel,z} dS \tag{6}$$

and

$$\dot{J} = \int_{r<r(U+K=0)} \rho_{\rm w} v_{\rm rel,z}^2 x dS, \tag{7}$$

respectively. Here, x is the projected length measured from the donor on to the orbital plane. $v_{\rm rel,\,z}$ is the normal component of the relative velocity vector to the S surface, and it is given in the procedure described in the Appendix.

From equations (6) and (7), the specific angular momentum of the accretion flow can be computed as

$$\ell = \dot{J}\,\dot{M}^{-1}. \tag{8}$$

3 Results

Next, we examine whether the accretion flow with the angular momentum obtained by our model can form an accretion disk. The accretion flow with its angular momentum ℓ will be circularized at the so-called circularization radius $r_{\rm circ}$ that is defined as

$$r_{\rm circ} = \frac{\ell^2}{GM_{\rm NS}}, \tag{9}$$

and this radius corresponds to the initial size of the accretion disk (Frank et al. 2002). If the accretion flow is captured by the magnetic field out of this radius, however, the flow cannot form an accretion disk and will fall along the field line towards the polar regions of the neutron star (Basko & Sunyaev 1976; Frank et al. 2002). Hence, to form an accretion disk, the above circularization radius should be larger than the radius at which the magnetic force becomes dominant (Frank et al. 2002):

$$r_{\rm m} = \left(\frac{B_{\rm NS}^4 r_{\rm NS}^{12}}{8\xi^2 GM_{\rm NS}\dot{M}^2}\right)^{1/7}. \tag{10}$$

This radius is called the magnetospheric radius. Here, ξ denotes the accretion efficiency, and this value is simply assumed to be 0.5 hereafter. At the same time, even if the circularization radius is larger than the magnetospheric radius, the mass accretion could be inhibited by the centrifugal force; this situation is known as the propeller phase (Illarionov & Sunyaev 1975; Stella et al. 1986). This condition is written as $r_{\rm m} > r_{\rm co}$, where the corotation radius $r_{\rm co}$ is

$$r_{\rm co} = \left(\frac{GM_{\rm NS} P_{\rm spin}^2}{4\pi^2}\right)^{1/3}. \tag{11}$$

This inhibition of the accretion will be maintained until the neutron star loses enough angular momentum and $r_{\rm co}$ becomes larger (Stella et al. 1986; Bozzo et al. 2008). In conclusion, the condition for the formation of an accretion disk in a wind-fed X-ray binary is

$$r_{\rm m} < r_{\rm co}, r_{\rm circ}. \tag{12}$$

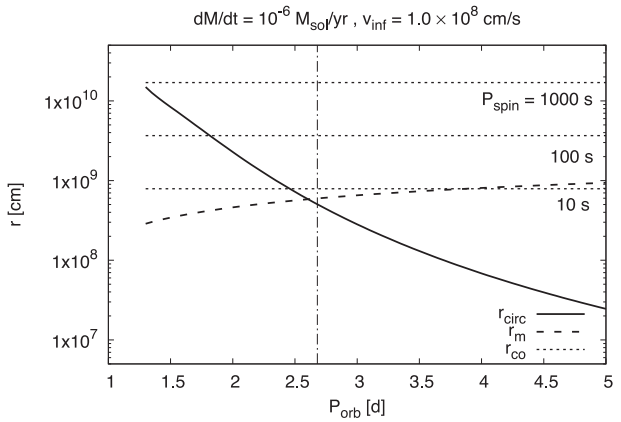

Fig. 3. Three radii, $r_{\rm circ}$, $r_{\rm m}$, and $r_{\rm co}$, are shown by solid, dashed, and dotted lines, respectively, as functions of the orbital period of the binary system. The co-rotation radii are shown for three cases: $P_{\rm spin} = 10$, 100, and 1000 s. The vertical line denotes the critical orbital period where the mass accretion rate becomes $\dot{M}_{\rm acc} = 4 \times 10^{16}$ g s^{-1}. Only to the left-hand-side of this vertical line could angular momentum be transported to the neighbor of the neutron star.

We investigate the condition where the above relation is satisfied, when we change various parameters.

In this study, we fix the mass, radius, and magnetic field of the neutron star as follows: $M_{\rm NS} = 1.4\,M_\odot$, $r_{\rm NS} = 1.0 \times 10^6$ cm, and $B_{\rm NS} = 2.0 \times 10^{12}$ G. Though the mass range of a neutron star is distributed between roughly 1.2 $M_\odot$ and $\sim 2\,M_\odot$, the mass of the neutron stars in HMXBs is not so far from 1.4 $M_\odot$ (Schwab et al. 2010; Falanga et al. 2015; Suwa et al. 2018). Also, the strength of the magnetic fields of neutron stars in HMXBs is concentrated around a few of 10^{12} G (Christodoulou et al. 2016; Taani et al. 2019). The wind velocity is computed by equation (3). First, to grasp the general tendencies, we assume the mass and radius of the donor as $M_{\rm d} = 15\,M_\odot$ and $R_{\rm d} = 10\,M_\odot$, respectively. However, later on, we use more realistic values when we make comparisons with the observed results.

With these settings, we vary the spin period of the neutron star $P_{\rm spin}$, the mass-loss rate of the donor $\dot{M}_{\rm w}$, the terminal velocity of the wind $v_{\rm inf}$, and the orbital period of the system $P_{\rm orb}$. As a typical result, in figure 3 we show the computed radii ($r_{\rm circ}$, $r_{\rm m}$, and $r_{\rm co}$) under the following parameter settings: $\dot{M}_{\rm w} = 1.0 \times 10^{-6}\,M_\odot$ yr^{-1}, $v_{\rm inf} = 1.0 \times 10^8$ cm s^{-1}. In this case, the maximum orbital period that satisfies the relationship in equation (12) is 2.6 d regardless of the spin period. We name this maximum orbital period where the condition of equation (12) is satisfied as $P_{\rm orb,\,max}$. In the present case, the lines of propeller limits are well above the magnetospheric radius in the region where $P_{\rm orb} < P_{\rm orb,\,max}$ is satisfied. In a system with a rapidly rotating neutron star, however, the disk formation condition could be limited by the propeller mass ejection (though fast-spinning neutron stars have not been found in wind-fed HMXBs).

Even if the condition in equation (12) is satisfied, the subsonic accretion shell might rearrange the angular momentum before the disk is formed, when the accretion rate is too small (Shakura et al. 2012). This critical mass accretion rate is given as

$$\dot{M}_{\rm acc} > 4 \times 10^{16}\ {\rm g\,s^{-1}}. \tag{13}$$

This limiting accretion rate for the shell forming is shown by a vertical dash–dotted line in figure 3. Only to the left-hand side of this vertical line is the mass accretion rate high enough that an accretion disk can be formed (see section 4). In the case shown in figure 3, the conditions of equations (12) and (13) are satisfied when the orbital period is shorter than 2.6 d.

In figure 4, we show the results obtained by changing parameters. Here, we vary the mass-loss rate of the donor ($\dot{M}_{\rm w} = 1.0 \times 10^{-5}$, 1.0×10^{-6} and $1.0 \times 10^{-7}\,M_\odot$ yr^{-1}) and the wind velocity ($v_{\rm inf} = 0.5$, 1.0 and 5.0×10^8 cm s^{-1}). In each case, we examine three spin periods of the neutron star ($P_{\rm spin} = 10$, 100, and 1000 s). When the wind velocity is slow ($v_{\rm inf} = 5 \times 10^7$ cm s^{-1}), the disk-forming condition, equation (12), is satisfied in broad range of $P_{\rm orb}$. However, when the mass-loss rate of the donor is small, the subsonic shell-forming condition, equation (13), dominates the possibility of the disk formation.

In figure 5, we show the maximum orbital period for the formation of an accretion disk, $P_{\rm orb,\,max}$, as functions of mass accretion rate and wind velocity. In this figure the mass-loss rate is chosen as a variable parameter and the results are shown for three different wind velocities. From the figure, we can see that the wind velocity causes a significant effect on the disk formation. When the wind velocity is large enough (say, $v_{\rm inf} > 1.0^8$ cm s^{-1}), the dependence of $P_{\rm orb,\,max}$ on the mass-loss rate is rather weak and the critical orbital period is quite short (less than 3 d, shorter than the typical period of HMXBs). On the other hand, when the wind velocity is slow, the dependence on the mass-loss rate becomes significant and the maximum orbital period becomes much longer when the mass-loss rate is large. The change of the gradient around $\dot{M}_{\rm w} \approx 1 \times 10^{-6}\,M_\odot$ yr^{-1}, in figure 5, stems from a change of the dominating conditions; below this point the shell-forming condition equation (13) limits the disk formation, while, on the other hand, when the mass-loss rate is larger than this point the disk formation is limited by the condition equation (12). These exchanges are shown by black dots in the figure.

The possibility of a disk formation around a compact object fed by slow wind has been previously suggested (Wang 1981; Shakura et al. 2012; El Mellah et al. 2019a; Taani et al. 2019). In Ducci et al. (2010), they considered the disk-forming possibility in SFXTs which are accreted

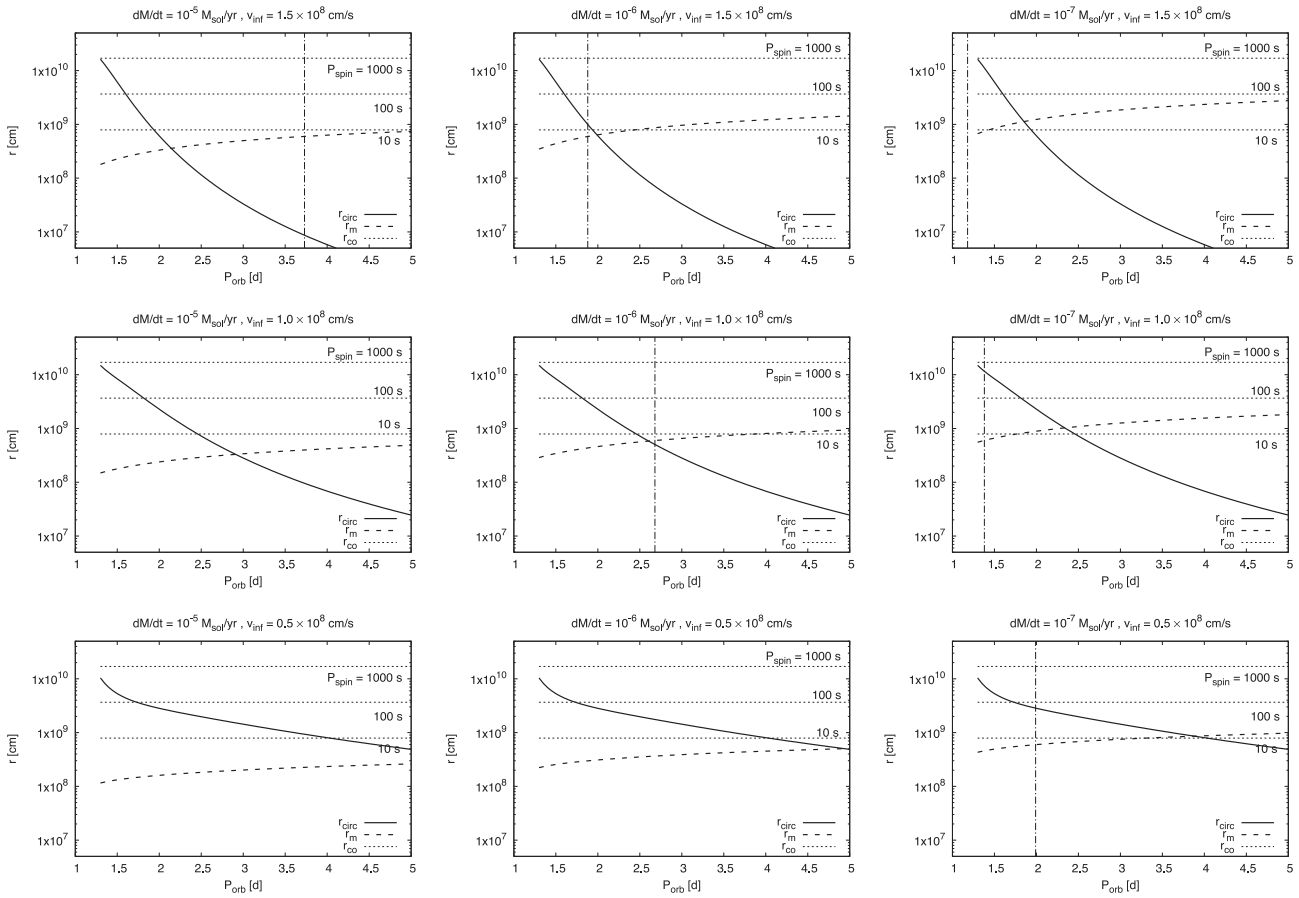

Fig. 4. Same as figure 3 but for different mass-loss rate and wind velocity. For the cases without vertical lines, the accretion rates are large enough in the entire parameter space.

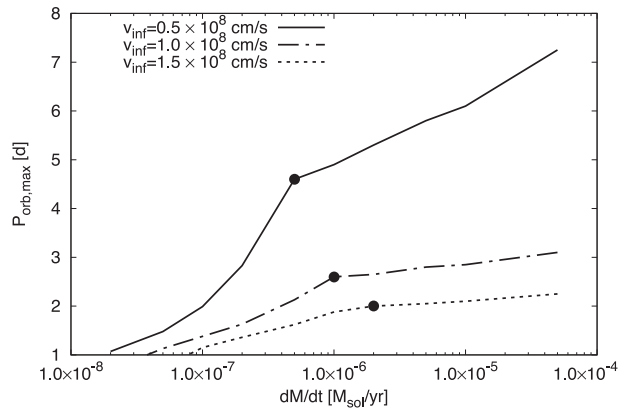

Fig. 5. The maximum orbital period to form an accretion disk, as a function of mass-loss rate of the donor. Results for three different $v_{\rm inf}$ are shown. The black dots indicate the change of which mechanism dominates the restriction of the disk formation..

by slow wind, to explain burst activities of SFXTs. In our treatment of a deformed accretion region (figure 2), we have found that further angular momentum could be transported and the possibility of disk formation becomes significant (this will be discussed further in section 4).

We can summarize our results as following:

- For systems with short orbital periods (for tight systems), the necessary condition for the disk formation ($r_{\rm m} < r_{\rm circ}$) could be satisfied.
- When the spin of the neutron star is fast, however, accretion could be inhibited due to the propeller effect. For a typical spin period of neutron stars in OB-HMXBs, however, it does not dominantly restrict the disk formation.
- When the wind velocity is slow, an accretion disk can be formed even in systems with large orbital period.
- When the mass-loss rate of the donor is large, an accretion disk can be formed even in systems with large orbital period. When the mass-loss rate of the donor is small, however, the disk formation could be limited by the subsonic shell-forming condition.

4 Discussion

4.1 Deformation of the accretion region

In this study, we have shown that even in a wind-accretion regime enough angular momentum to form an accretion

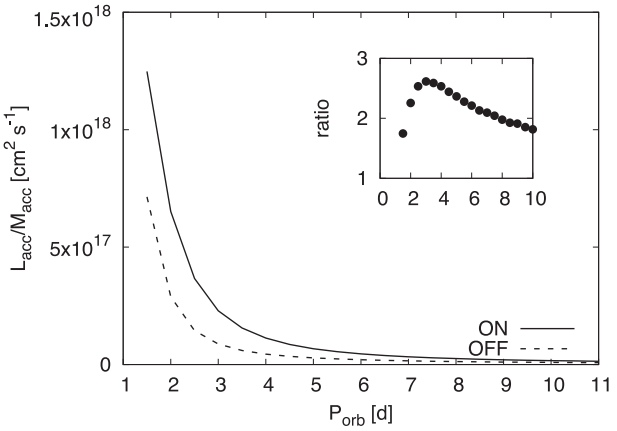

Fig. 6. The transported specific angular momentum, shown when the deformation of the accretion region is considered (ON) and when it is not (OFF). In the small box, the ratio of this specific angular momentum ($\ell_{\rm ON}/\ell_{\rm OFF}$)as a function of the orbital period is shown. The parameters of the system are the same as in the case shown in figure 3.

disk is transported. Furthermore, we have shown that it is crucial to consider the orbital motion of the neutron star and the acceleration of the wind matter. If we consider these two effects, the accretion region shifts inwards of the orbit as shown in figure 2. Because of this shift of accretion region, the neutron star can capture an extra dense wind matter from the inner region. This makes it possible to capture a large amount of angular momentum from the wind. At the same time, it could be understood from figure 2 that though the wind matter accreted from the outer region has a large velocity, its density is much lower and the accretion region is rather narrower. Namely, the inward deformation of the accretion region is essentially important in estimating the accretion rate of the angular momentum.

In order to depict the effect of the deformation of the accretion region clearly, an illustration of the result is given in figure 6, where the transported specific angular momentum is shown in two cases. For the first case, the deformation of the accretion region is not considered. This is the case which is shown by the dashed curve in figure 2, and we refer this case as OFF. On the other hand, the result obtained with the consideration of the deformed accretion region is shown at the same time by the solid curve. This second case corresponds to the accretion region shown by the solid line in figure 2. We refer this second case as ON. Clearly, in the ON case, the accreted specific angular momentum increases. Though this deformation effect has been considered less serious in previous works (Hoyle & Lyttleton 1939; Shapiro & Lightman 1976; Wang 1981), this result shows that the deformation could play a rather important role in the nature of the accretion mode in tight binary systems.

At the same time, in the small box of figure 6, we show the ratio of the specific angular momentum between these two cases as a function of the orbital period. In the present parameter set, this ratio takes maximum at $P_{\rm orb} = 3$ d. This behavior could be understood as follows. When the orbital period is long (i.e., orbital separation is large), the wind from the donor has already significantly accelerated ($v_{\rm w} = v_{\rm inf} \gg v_{\rm orb}$). Hence, the wind could be considered like a planar uniform flow. Then, the effect of the deformation of the accretion region could be smaller. On the other hand, when the orbital separation is small, the orbital velocity dominates the relative velocity. Therefore, the acceleration of the wind does not have an important role. In conclusion, the deformation of the accretion region becomes important at the intermediate orbital period around 3 d.

4.2 Formation of accretion disk

Figure 5 indicates that an accretion disk could be formed even when the orbital period of the system is rather large, if the wind velocity is slow. The slow wind velocity is caused by slow terminal velocity due to certain reasons such as line-driven efficiency and X-ray photo-dissociations (Ducci et al. 2010; Krtička et al. 2012; Karino 2014). At the same time, wind velocity also becomes slower due to the increase of the relative radius of the donor to the orbital radius, as seen in equation (3). In the above discussion, however, we have only shown that a certain amount of angular momentum could be transported inside the accretion radius. Deep inside the accretion radius, it is necessary to consider whether an accretion disk could really be formed or not.

In general, the captured matter from the stellar wind forms a shock during its falling path to the neutron star. If the cooling is ineffective, falling matter could form a quasi-static settling shell below the shock (Shakura et al. 2012). Once such a shell is formed, the angular momentum is transported due to turbulence caused by hydrodynamic instabilities inside the shell. Hence, the transported angular momentum will be redistributed before it reaches deep inside the accretion radius. When the accretion rate is large enough, $\dot{M} > 4 \times 10^{16}\,{\rm g\,s^{-1}}$, however, a settling shell is not formed and accretion matter could fall on to the neutron star quickly. This limiting accretion rate for the shell forming is shown by the vertical dash–dotted line in figures 3 and 4. This line shows the limiting case where the mass accretion rate evaluated by equation (6) becomes the critical value: $4 \times 10^{16}\,{\rm g\,s^{-1}}$. To the right-hand side of this vertical line, a quasi-spherical subsonic shell will be formed and the accreted angular momentum will be redistributed in the shell. In this case, therefore, axisymmetry recovers and the accretion disk cannot be formed. On the other hand, to the left-hand side of the vertical line the mass accretion

rate is high enough and a settling shell cannot be formed. Then the angular momentum will be transported to deep inside the accretion region. Finally, if the condition given by equation (12) is satisfied, an accretion disk would be formed.

The above condition on the mass accretion rate is also important when considering the nature of the formed accretion disk. When the mass supply is small, the accretion disk would be a radiatively inefficient accretion flow (RIAF), and its X-ray luminosity would steeply decrease with mass accretion rate (Narayan & Yi 1994, 1995; Kato et al. 2008). The accretion disk will be RIAF-like only when the accretion rate is quite low and the temperature is high. Hence, if our disk formation condition is satisfied (high accretion rate), it seems reasonable that a disk would form which behaves as a standard disk (Shakura & Sunyaev 1973). We hope future observations with more sensitive techniques can test this possibility.

To fix the position of the inner edge of the accretion disk, the effect of the magnetic field is crucially important. Moreover, the neutron star magnetosphere plays an important role in the onset of the propeller mass ejection (Stella et al. 1986; Bozzo et al. 2008). In this study, we assume a constant magnetic field strength; $B = 2 \times 10^{12}$ G. Actually, the neutron star magnetic field strength could take the value from the lower limit ($\sim 10^{9}$ G) seen in LMXB systems to the higher end ($\sim 10^{14}$ G) observed in magnetars (Pfahl et al. 2002; Podsiadlowski et al. 2004; van den Heuvel 2009): it spans five orders of possiblities. According to the straightforward observations of cyclotron resonance features in HMXB systems, however, most neutron stars in HMXBs show an intermediate level of field strength, $\sim 10^{12}$ G (Taani et al. 2018, 2019). Although this stems from a certain observational bias, it is worth mentioning that the magnetic fields are still $\sim 10^{13}$ G even in the most active neutron X-ray sources such as LMC X-4 and NGC300 ULX-1 (Moon & Eikenberry 2001; Moon et al. 2003; Levine et al. 2000; Carpano et al. 2018). Therefore our assumed magnetic field of 2×10^{12} G is not an odd choice for a first attempt.

Considering a system which has an orbital period slightly shorter than the critical period, $P_{\rm orb,\,max}$, the difference between two radii ($r_{\rm m}$ and $r_{\rm circ}$) in such a system is small, and the size of the formed disk may be very small. Once an accretion disk is formed, however, due to viscous effects the angular momentum of the disk matter could be transported from inside towards the outer edge. At the same time, the matter near the outer edge would be pushed out and the disk itself would expand. At the expanded disk edge, subsequent accreted matter will be attached and the size of the disk would be further extended. For example, the wind-fed HMXB system LMC X-4 has a warped accretion disk large enough to shade the X-ray from the neutron star, even

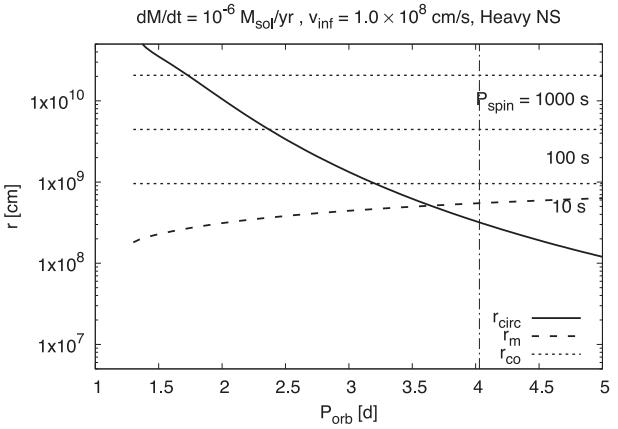

Fig. 7. Same as figure 3 but for a heavy NS: $M_{\rm NS} = 2.5\,M_{\odot}$. The other parameters are the same as in figure 3. The maximum orbital period, $P_{\rm orb,\,max}$, is extended up to 3.5 d.

though it is expected that $r_{\rm circ} \approx r_{\rm m}$ and the disk size could be small (this is discussed later).

In observed systems, the orbital eccentricities are not exactly zero. The eccentricity changes the geometrical relation of the neutron star to the stellar wind and affects the results. In typical Be-type HMXBs, the orbital eccentricity is rather large; it is considered to be induced by the natal kick when the neutron star was born in a core-collapse supernova. On the other hand, however, an OB-type HMXB typically has small ($e < 0.1$) eccentricity (Bildsten et al. 1997). This is because of the strong circularizing effect caused by the interaction between the neutron star and dense wind matter. The circularizing time could be much smaller than the HMXB life-time. Hence, in the present situations, we could neglect the effect of such orbital eccentricities.

4.3 Diversity of the donor and neutron star

In this study, we have considered only a typical neutron star whose mass is 1.4 $M_{\odot}$. Recent studies have shown, however, that some neutron stars have larger mass, up to 2 $M_{\odot}$ (van Kirkwijk et al. 1995; Rawls et al. 2011; Falanga et al. 2015). Such heavy neutron stars made a strong constraint on the equation of state of the neutron stellar matter and play an important role in understanding the nature of condensed matter. In the present study, such a large mass of the neutron star also changes the geometry of the accretion region. Deep potential of a heavy neutron star broadens the accretion radius, especially in slow wind side, and enhances the asymmetry of the wind geometry. This asymmetric wind brings further extra angular momentum to the neutron star neighbor and relaxes the condition of disk formation. In order to evaluate this effect, we show the result for a heavy neutron star with $M_{\rm NS} = 2.5\,M_{\odot}$ in figure 7. In this example, the other conditions are the same as in the case shown in

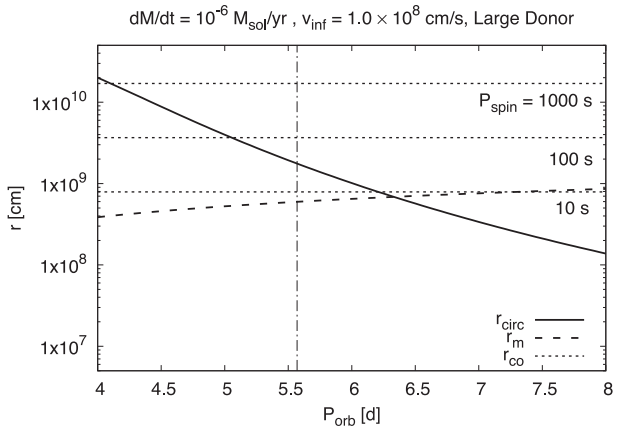

Fig. 8. Same as figure 3 but for a large donor: $R_{\rm d} = 20\,R_\odot$. The other parameters are the same with figure 3. The maximum orbital period, $P_{\rm orb,\,max}$, is limited at 5.3 d due to subsonic shell formation.

figure 3. The maximum orbital period, $P_{\rm orb,\,max}$, is extended up to 3.5 d in this case. Since the mass of the neutron star cannot largely exceed 2 $M_\odot$, we can conclude that the effect of the neutron stellar mass could be limited in the present context.

We have considered only a typical super-giant (SG) donor with $M_{\rm d} = 15\,M_\odot$ and $R_{\rm d} = 10\,R_\odot$. The wind velocity at the neutron star position, however, depends on the donor size [see equation (3)]. That is, when the donor size is large, the wind velocity becomes slower since the zone of acceleration effectively decreases. As a consequence, the possibility of disk formation could be larger. To confirm the effect of donor size, we have additionally computed the same case study for a large donor with $R_{\rm d} = 20\,R_\odot$. The result is shown in figure 8. In this case, the parameters except for the donor radius are the same as in the case of figure 3. We can see that, in this case, the condition of equation (12) is satisfied in a broader range $P_{\rm orb} < 6.4$ d for all spin periods. This time, however, the limit of subsonic shell formation dominates the maximum orbital period for disk formation. As a result, a system with an orbital period of less than 5.3 d could form an accretion disk around the neutron star. This limit will be pushed up due to the high mass-loss rate of the donor (see figure 4). Since a large evolved star tends to increase its mass-loss rate at the same time, an evolved donor would have a large possibility of forming an accretion disk around the neutron star.

4.4 Observed systems

4.4.1 LMC X-4

LMC X-4 is one of the most powerful persistent OB-type X-ray binaries in our neighborhood. It emits luminous X-rays with $L_{\rm X} = 3$–$4 \times 10^{38}\,{\rm erg\,s^{-1}}$ persistently, and often causes bright X-ray flares achieving $L_{\rm X} \sim 10^{40}\,{\rm erg\,s^{-1}}$, which exceeds the Eddington limit (Moon et al. 2003; Shtykovsky et al. 2018). The spin period, orbital period, and orbital eccentricity are 13.5 s, 1.4 d, and <0.003, respectively (Li et al. 1978; White 1978; Kelley et al. 1983). From the spectral properties, the donor star is identified as an O8III type super-giant star, the mass of which is assumed to be $M_{\rm d} = 18\,M_\odot$ (Chevalier & Ilovaisky 1977; Falanga et al. 2015). Besides the orbital period, it shows 30.5-d periodicity and this super-orbital periodicity is suggested to be caused by a warped accretion disk around the neutron star (Ilovaisky et al. 1984; Levine et al. 1991).

Table 1. Important parameters of HMXB systems: LMC X-4 and OAO 1657−415.*

Name	LMC X-4	OAO 1657−415
$M_{\rm d}$ [$M_\odot$]	18	17.5
$R_{\rm d}$ [$R_\odot$]	7.7	25
$P_{\rm spin}$ [s]	13.5	37.7
$P_{\rm orb}$ [d]	1.4	10.4
$v_{\rm inf}$[10^8 cm s^{-1}]	0.5	0.25
$\dot{M}_{\rm d}$[$10^{-6}\,M_\odot$ yr^{-1}]	50	2
$B_{\rm NS}$[10^{12} G]	11.2	4

*The binary parameters that we have used in the analysis. References are in the text.

In this bright system, since the existence of the accretion disk around the neutron star is evident, it has been considered that the accretion matter is supplied via RLOF (Levine et al. 2000; Preciado et al. 2002). Recent analysis, however, reveal that the radius of the donor remains confined to 7–8 $R_\odot$ (Rawls et al. 2011; Falanga et al. 2015). Assuming that the neutron star mass is 1.4 $M_\odot$, the Roche lobe size is much larger than the donor radius. Hence, the donor could remain well inside the lobe and RLOF has not been started. On the other hand, the ejection of strong wind from the donor has also been suggested (Vrtilek et al. 1997; Boroson et al. 1999). Thus wind-fed accretion in this system is suspected.

Given these circumstances, we consider the possibility of the disk formation due to angular momentum accretion via stellar wind in this system. For this purpose, we use the same analysis described in the previous sections. The parameters used are summarized in table 1. The corresponding radii ($r_{\rm circ}$, $r_{\rm m}$, and $r_{\rm co}$) are shown in figure 9. From the condition, equation (12), in this system, disk formation via stellar wind could be possible if the orbital period is shorter than 2.5 d. Since the orbital period of this system is 1.4 d, and since the propeller effect could be avoided with its orbital period, it is strongly suggested that disk formation via wind accretion could be possible.

Additionally, in this system, the difference between $r_{\rm circ}$ and $r_{\rm m}$ is rather small. It means that the accretion

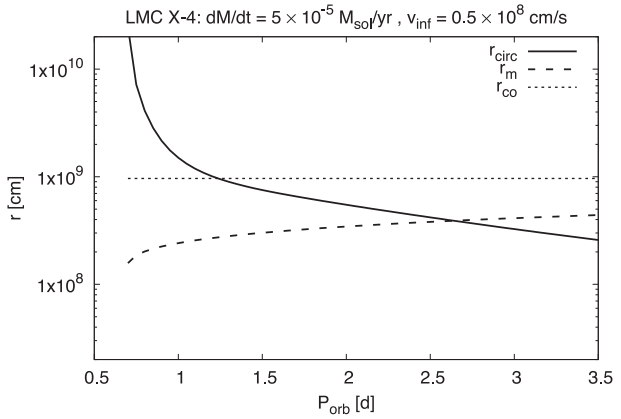

Fig. 9. This is the figure for LMC X-4. The binary parameters are summarized in table 1.

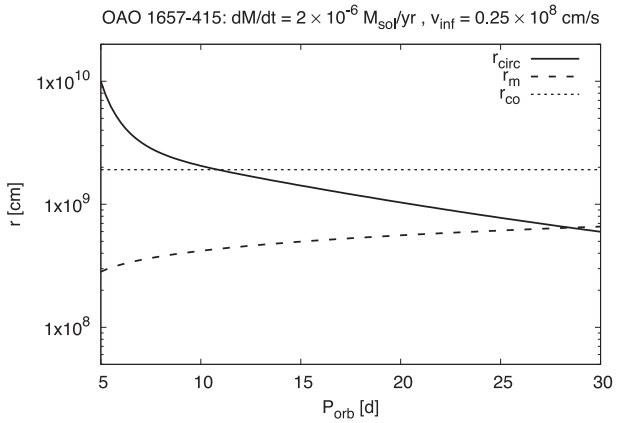

Fig. 10. Results of each radii computed with the parameters of OAO 1657−415. The binary parameters are summarized in table 1.

regime (direct wind accretion/disk accretion) could be converted easily if the situation varies. Observation shows that this system fluctuates between the spin-up and spin-down regime (Molkov et al. 2017). Such a spin evolution might be related to such a marginal situation. Since the exchange of accretion regime may change the spectral feature, multifaceted studies are highly necessary (Paul et al. 2002; Naik & Paul 2003).

4.4.2 OAO 1657−415

OAO 1657−415 was identified in the 1970s, and has been one of the most famous HMXBs. The orbital period and orbital eccentricity are 10.448 d and 0.107, respectively (Chakrabarty et al. 1993). The donor star was identified as an Ofpe star, however, since the hydrogen line is weak, it might be a Wolf–Rayet star, like Cyg X-3 (Mason et al. 2012). From optical observations, the parameters of the donor have been measured as $M_{\rm d} = 14.3\,M_{\odot}$, $R_{\rm d} = 24.8\,R_{\odot}$, and $\dot{M}_{\rm w} = 2 \times 10^{-6}\,M_{\odot}\,{\rm yr}^{-1}$ (Mason et al. 2012). The wind velocity is suggested to be very slow ($v_{\rm inf} = 2.5 \times 10^{7}\,{\rm cm\,s}^{-1}$), and it may be due to a displacement from spherical symmetry caused by a neutron star. It is known that the standard binary evolution scenario cannot derive such a set of binary parameters for this system (Molteni et al. 2001; Mason et al. 2012). Although no firm evidence of an accretion disk has been reported, the shape of the cumulative luminosity distribution of this system is similar to disk-forming systems (Sidoli & Paizis 2018).

We apply our model to this system with the same procedure that is discussed above. (Since the radius of the donor and the size of the Roche lobe size is almost the same in this system, it is a sensitive issue whether RLOF proceeds or not.) The results of each radii computed with the parameters of OAO 1657−415 are shown in figure 10. From this figure, if the orbital period is shorter than 23 d, the disk formation could be possible. In fact, the orbital period of this system is 10.4 d and it clearly satisfies this condition. Also, we can see that the propeller effect and subsonic shell forming do not work in this parameter range. Therefore, we conclude that the disk formation could also be realized in this system via wind-fed accretion.

In this system, the slow wind (due to slow wind and large donor size) plays an important role in the disk formation. Such a disk formation in slow-wind binary is also suggested by numerical computations (Huarte-Espinosa et al. 2013), and this consistency supports the robustness of our working hypotheses.

Very recently, it has been reported that a disk-like structure could be formed even when the donor does not fill its Roche lobe under certain conditions, according to the numerical computations (El Mellah et al. 2019a, 2019b). Such a marginal accretion mode (wind RLOF/beamed wind) might be a key to understanding the diversity and complexity of HMXBs.

5 Conclusion

In this study, we have revisited to the transportation rate of the angular momentum in the wind-fed neutron star X-ray binaries. We have taken into account the asymmetry due to the orbital motion of the neutron star and the wind acceleration. The asymmetry of the wind can lead to a deformation of the accretion region, and due to this a large amount of angular momentum could be transported inside the accretion radius even in wind accretion. Furthermore, we have shown that an accretion disk could be formed around the neutron star under certain situations; when the wind velocity is slow because of a small terminal velocity and/or inefficient wind acceleration due to a large donor radius, the possibility of disk formation could be larger.

We applied our disk-formation criteria to the observed peculiar systems hitherto considered to be fed via

RLOF. In our analysis, neutron stars in LMC X-4 and OAO 1657−415 could have accretion disks, even if they were fed via stellar winds. For LMC X-4, the orbital period is short enough to capture plenty of angular momentum from the wind of the donor. In addition, the propeller effect could be avoided with this orbital period. This results elucidates the source of a warped accretion disk in this object. For OAO 1657−415, the slow wind enhances the transportation rate of the angular momentum and gains the possibility of the disk formation.

Finally, the existence of an accretion disk will affect the observed properties such as spectral hardness and the spin evolution of the accreting neutron star. To reveal the accretion nature of HMXBs, further studies both in observations and on the theoretical side are required.

Acknowledgments

We thank the referee for fruitful suggestions. This work was supported by JSPS KAKENHI Grant Number 18K03706. Ali Taani gratefully acknowledges the Institute of High Energy Physics, Chinese Academy of Sciences through CAS-PIFI Fellowship 2018.

Appendix. Tips of computation

Here, the coordinate system which we have used to evaluate the accretion rate of angular momentum via line-driven stellar wind is described. At the beginning, we define a reference surface S of the wind accretion to evaluate the accreted angular momentum. We find the relative velocity vector of the wind at the position of the neutron star, $\boldsymbol{v}_{\rm rel}$. The relative velocity can be obtained by a simple addition of the orbital velocity $\boldsymbol{v}_{\rm orb} = v_{\rm orb}\boldsymbol{e}_{\rm T}$ [see, equation (2)] and the wind velocity $\boldsymbol{v}_{\rm w} = v_{\rm w}\boldsymbol{e}_{\rm R}$ [see, equation (3)]. Then, we set a surface which normal vector coincides with $\boldsymbol{v}_{\rm rel}$. We consider an accretion region in this surface and estimate the mass and angular momentum transported to the neighbor of the neutron star.

Now we set the x-axis on the line of intersection between the S plane and the orbital plane. Then, the x-direction is inclined to the relative velocity vector by the angle θ given as

$$\theta = \frac{\pi}{2} - \tan^{-1}\left(\frac{v_{\rm w}}{v_{\rm orb}}\right). \tag{A1}$$

We set the z-direction as the direction of the relative velocity of the wind at the neutron star position. For x- and z-axes, we set the positive direction as the direction receding away from the donor. Additionally, we set the y-direction as $\boldsymbol{e}_{\rm z} = \boldsymbol{e}_{\rm x} \times \boldsymbol{e}_{\rm y}$, where $\boldsymbol{e}_{\rm x,y,z}$ denotes the unit vectors in each direction. This situation is depicted in figure 11.

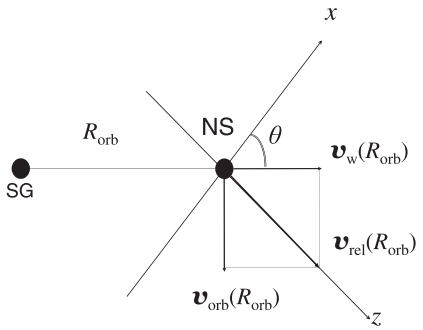

Fig. 11. The set-up concept of axes. The wind, orbital, and relative velocity vectors are those at the neutron star position.

On the S plane (x–y plane), the relative velocity of the wind is obtained as

$$v_{\rm rel}(x, y) = \left[v_{\rm w}(R')^2 + v_{\rm orb}(R)^2\right]^{1/2}, \tag{A2}$$

where R' is the distance from the center of the donor:

$$R' = \sqrt{R(x, 0)^2 + y^2}. \tag{A3}$$

The value of R on the x-axis, $R(x)$, could be obtained as

$$R^2 = R_{\rm orb}^2 + x^2 - 2R_{\rm orb}x\cos(\pi - \theta). \tag{A4}$$

Under such a setting of the coordinate system, we evaluate the balance between wind kinetic energy and the neutron star potential, and find the accretion region. In our x–y coordinate system, the potential of the neutron star can be described as

$$U = -\frac{GM_{\rm NS}}{\sqrt{x^2 + y^2}}, \tag{A5}$$

and the kinetic energy of the wind can be written as

$$K = \frac{1}{2}v_{\rm rel}(x, y)^2. \tag{A6}$$

The wind matter passing each point on the S surface, (x, y), will be trapped by the neutron star if $K + U < 0$. Making the dependence on the $x - y$ coordinate clear, equations (6) and (7) can be written as

$$\dot{M} = \int_{K+U<0} \rho_{\rm w}(x, y)v_{\rm rel,z}(x, y)dxdy, \tag{A7}$$

and

$$\dot{J} = \int_{K+U<0} \rho_{\rm w}(x, y)v_{\rm rel,z}(x, y)^2 x dxdy, \tag{A8}$$

respectively. $v_{\rm rel,\,z}(x, y)$ is the z-component of the relative velocity vector of the wind at the point (x, y) (namely, the

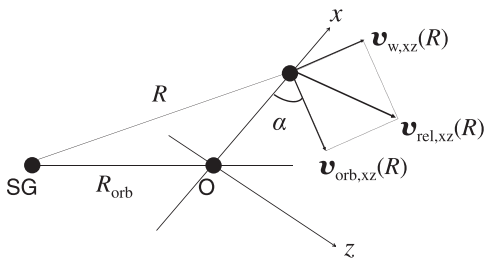

Fig. 12. Definition of angles. The wind, orbital, and relative velocity vectors are projected on the *x*–*z* plane.

normal component to the *S* plane), and it is given as the following;

$$v_{\rm rel,z} = \frac{v_{\rm w} R}{R'} \sin\left(\frac{\pi}{2} - \alpha\right) + |\boldsymbol{v}_{\rm orb}| \sin\beta. \tag{A9}$$

α is the angle between the relative velocity vector of the wind at the position (x, y) and the reference plane *S*, which is given by

$$\alpha = \frac{\pi}{2} - \cos^{-1}\left(\frac{R^2 + x^2 - R_{\rm orb}^2}{2Rx}\right) \tag{A10}$$

(see figure 12).

References

Bachetti, M., et al. 2014, Nature, 514, 202
Basko, M. M., & Sunyaev, R. A. 1976, MNRAS, 175, 395
Bhattacharya, D., & van den Heuvel, E. P. J. 1991, Phys. Rev., 203, 1
Bildsten, L., et al. 1997, ApJS, 113, 367
Blondin, J. M. 2013, ApJ, 767, 135
Blondin, J. M., & Pope, T. C. 2009, ApJ, 700, 95
Bondi, H., & Hoyle, F. 1944, MNRAS, 104, 273
Boroson, B., Kallman, T., McCray, R., Vrtilek, S. D., & Raymond, J. 1999, ApJ, 519, 191
Bozzo, E., Falanga, M., & Stella, L. 2008, ApJ, 683, 1031
Carpano, S., Haberl, F., Maitra, C., & Vasilopoulos, G. 2018, MNRAS, 476, L45
Castor, J. I., Abbott, D. C., & Klein, R. I. 1975, ApJ, 195, 157
Chakrabarty, D., et al. 1993, ApJ, 403, L33
Chevalier, C., & Ilovaisky, S. A. 1977, A&A, 59, L9
Christodoulou, D. M., Laycock, S. G. T., Yang, J., & Fingerman, S. 2016, ApJ, 829, 30
Corbet, R. H. D. 1984, A&A, 141, 91
Corbet, R. H. D. 1986, MNRAS, 220, 1047
Davies, R. E., & Pringle, J. E. 1981, MNRAS, 196, 209
Ducci, L., Sidoli, L., & Paizis, A. 2010, MNRAS, 408, 1540
Edgar, R. 2004, New Astron. Rev., 48, 843
Eggleton, P. 2006, Evolutionary Processes in Binary and Multiple Stars (Cambridge: Cambridge University Press)
Ekşi, K. Y., Andaç, errorIdot. C., Çıkıntoğlu, S., Gençali, A. A., Güngör, C., & Öztekin, F. 2015, MNRAS, 448, L40
El Mellah, I., & Casse, F. 2017, MNRAS, 467, 2585
El Mellah, I., Sander, A. A. C., Sundqvist, J. O., & Keppens, R. 2019a, A&A, 622, A189
El Mellah, I., Sundqvist, J. O., & Keppens, R. 2019b, A&A, 622, L3
Falanga, M., Bozzo, E., Lutovinov, A., Bonnet-Bidaud, J. M., Fetisova, Y., & Puls, J. 2015, A&A, 577, A130
Foglizzo, T., & Ruffert, M. 1997, A&A, 320, 342
Frank, J., King, A., & Raine, D. J. 2002, Accretion Power in Astrophysics, 3rd ed. (Cambridge: Cambridge University Press)
Fryxell, B. A., & Taam, R. E. 1988, ApJ, 335, 862
Fürst, F., et al. 2016, ApJ, 831, L14
Giménez-García, A., et al. 2016, A&A, 591, A26
Hadrava, P., & Čechura, J. 2012, A&A, 542, A42
Hoyle, F., & Lyttleton, R.A. 1939, Math. Proc. Cambridge Phil. Soc., 35, 405
Huarte-Espinosa, M., Carroll-Nellenback, J., Nordhaus, J., Frank, A., & Blackman, E. G. 2013, MNRAS, 433, 295
Illarionov, A. F., & Sunyaev, R. A. 1975, A&A, 39, 185
Ilovaisky, S. A., Chevalier, C., Motch, C., Pakull, M., van Paradijs, J., & Lub, J. 1984, A&A, 140, 251
in't Zand, J. J. M. 2005, A&A, 441, L1
Israel, G. L., et al. 2017a, MNRAS, 466, L48
Israel, G. L., et al. 2017b, Science, 355, 817
Jahanara, B., Mitsumoto, M., Oka, K., Matsuda, T., Hachisu, I., & Boffin, H. M. J. 2005, A&A, 441, 589
Karino, S. 2014, PASJ, 66, 34
Kato, S., Mineshige, S., & Fukue, J. 2008, Black-Hole Accretion Disks (Kyoto: Kyoto University Press)
Kelley, R. L., Jernigan, J. G., Levine, A., Petro, L. D., & Rappaport, S. 1983, ApJ, 264, 568
Krtička, J., Kubát, J., & Skalický, J. 2012, ApJ, 757, 162
Kudritzki, R.-P., & Puls, J. 2000, ARA&A, 38, 613
Levine, A. M., Rappaport, S. A., Putney, A., Corbet, A., & Nagase, F. 1991, ApJ, 381, 101
Levine, A. M., Rappaport, S. A., & Zojcheski, G. 2000, ApJ, 541, 194
Li, F., Rappaport, S., & Epstein, A. 1978, Nature, 271, 37
Liu, Z.-W., Stancliffe, R. J., Abate, C., & Matrozis, E. 2017, ApJ, 846, 117
Mason, A. B., Clark, J. S., Norton, A. J., Crowther, P. A., Tauris, T. M., Langer, N., Negueruela, I., & Roche, P. 2012, MNRAS, 422, 199
Matsuda, T., Inoue, M., & Sawada, K. 1987, MNRAS, 226, 785
Matsuda, T., Sekino, N., Sawada, K., Shima, E., Livio, M., Anzer, U., & Boerner, G. 1991, A&A, 248, 301
Molkov, S., Lutovinov, A., Falanga, M., Tsygankov, S., & Bozzo, E. 2017, MNRAS, 464, 2039
Molteni, D., Kuznetsov, O. A., Bisikalo, D. V., & Boyarchuk, A. A. 2001, MNRAS, 327, 1103
Moon, D.-S., & Eikenberry, S. S. 2001, ApJ, 549, L225
Moon, D.-S., Eikenberry, S. S., & Wasserman, I. M. 2003, ApJ, 586, 1280
Naik, S., & Paul, B. 2003, A&A, 401, 265
Narayan, R., & Yi, I. 1994, ApJ, 428, L13
Narayan, R., & Yi, I. 1995, ApJ, 452, 710
Paul, B., Nagase, F., Endo, T., Dotani, T., Yokogawa, J., & Nishiuchi, M. 2002, ApJ, 579, 411
Pfahl, E., Rappaport, S., Podsiadlowski, P., & Spruit, H. 2002, ApJ, 574, 364

Podsiadlowski, P., Langer, N., Poelarends, A. J. T., Rappaport, S., Heger, A., & Pfahl, E. 2004, ApJ, 612, 1044
Postnov, K., Oskinova, L., & Torrejón, J. M. 2016, in 11th INTEGRAL conference gamma-ray astrophysics in multi-wavelength perspective, PoS(INTEGRAL2016), 029
Preciado, M. E., Boroson, B., & Vrtilek, S. D. 2002, PASP, 114, 340
Rawls, M. L., Orosz, J. A., McClintock, J. E., Torres, M. A. P., Bailyn, C. D., & Buxton, M. M. 2011, ApJ, 730, 25
Ruffert, M. 1997, A&A, 317, 793
Ruffert, M. 1999, A&A, 346, 861
Ruffert, M., & Anzer, U. 1995, A&A, 295, 108
Schwab, J., Podsiadlowski, P., & Rappaport, S. 2010, ApJ, 719, 722
Shakura, N., Postnov, K., Kochetkova, A., & Hjalmarsdotter, L. 2012, MNRAS, 420, 216
Shakura, N., Postnov, K., Sidoli, L., & Paizis, A. 2014, MNRAS, 442, 2325
Shakura, N. I., & Sunyaev, R. A. 1973, A&A, 24, 337
Shapiro, S. L., & Lightman, A. P. 1976, ApJ, 204, 555
Shtykovsky, A. E., Arefiev, V. A., Lutovinov, A. A., & Molkov, S. V. 2018, Astron. Lett., 44, 149
Sidoli, L., & Paizis, A. 2018, MNRAS, 481, 2779
Soker, N. 2004, MNRAS, 350, 1366
Stella, L., White, N. E., & Rosner, R. 1986, ApJ, 308, 669
Suwa, Y., Yoshida, T., Shibata, M., Umeda, H., & Takahashi, K. 2018, MNRAS, 481, 3305
Taani, A., Karino, S., Song, L., Al-Wardat, M., Khasawneh, A., & Mardini, M. K. 2019, Res. Astron. Astrophys., 19, 12
Taani, A., Karino, S., Song, L., Zhang, C., & Chaty, S. 2018, arXiv:1808.05345
Theuns, T., & Jorissen, A. 1993, MNRAS, 265, 946
van den Heuvel, E. P. J. 2009, in Physics of Relativistic Objects in Compact Binaries: From Birth to Coalescence, ed. M. Colpi et al. (Dordrecht: Springer), 125
van der Meer, A., Kaper, L., van Kerkwijk, M. H., Heemskerk, M. H. M., & van den Heuvel, E. P. J. 2007, A&A, 473, 523
van Kerkwijk, M. H., van Paradijs, J., Zuiderwijk, E. J., Hammerschlag-Hensberge, G., Kaper, L., & Sterken, C. 1995, A&A, 303, 483
Vrtilek, S. D., Boroson, B., Cheng, F. H., McCray, R., & Nagase, F. 1997, ApJ, 490, 377
Walter, R., Lutovinov, A. A., Bozzo, E., & Tsygankov, S. S. 2015, A&AR, 23, 2
Walter, R., & Zurita Heras, J. 2007, A&A, 476, 335
Wang, Y.-M. 1981, A&A, 102, 36
White, N. E. 1978, Nature, 271, 38